Hydrol. Earth Syst. Sci. Discuss., doi:10.5194/hess-2015-408, 2016
Manuscript under review for journal Hydrol. Earth Syst. Sci.
Published: 15 January 2016

Hydrology and Earth System Sciences
Open Access
Discussions

Sensitivity of future water availability projections to Global Climate Model, evapotranspiration estimation method, and greenhouse gas emission scenario

S. Chang[1], W. Graham[1,2], S. Hwang[3], and R. Muñoz-Carpena[1]

[1]Department of Agricultural and Biological Engineering, University of Florida, 570 Weil Hall, P.O. Box 116601, Gainesville, FL 32611-6601, USA
[2]Water Institute, University of Florida, 570 Weil Hall, P.O. Box 116601, Gainesville, FL 32611-6601, USA
[3]Department of Agricultural Engineering, Gyeongsang National University, Jinju, South Korea

Received: 23 September 2015 – Accepted: 2 December 2015 – Published: 15 January 2016

Correspondence to: S. Chang (swjason@ufl.edu)

Published by Copernicus Publications on behalf of the European Geosciences Union.

Abstract

Projecting water availability under various possible future climate scenarios depends on the choice of Global Climate Model (GCM), evapotranspiration (ET) estimation method and Representative Concentration Pathway (RCP) trajectory. The relative contribution of each of these factors must be evaluated in order to choose an appropriate ensemble of future scenarios for water resources planning. In this study variance-based global sensitivity analysis and Monte Carlo filtering were used to evaluate the relative sensitivity of projected changes in precipitation (P), ET and water availability (defined here as P–ET) to choice of GCM, ET estimation method and RCP trajectory over the continental United States (US) for two distinct future periods: 2030–2060 (future period 1) and 2070–2100 (future period 2). A total of 9 GCMs, 10 ET methods and 3 RCP trajectories were used to quantify the range of future projections and estimate the relative sensitivity of future projections to each of these factors. In general, for all regions of the US, changes in future precipitation are most sensitive to the choice of GCM, while changes in future ET are most sensitive to the choice of ET estimation method. For changes in future water availability, the choice of GCM is the most influential factor in the cool season (December–March) and the choice of ET estimation method is most important in the warm season (May–October) for all regions except the South East US where GCM and ET have approximately equal influence throughout most of the year. Although the choice of RCP trajectory is generally less important than the choice of GCM or ET method, the impact of RCP trajectory increases in future period 2 over future period 1 for all factors. Monte Carlo filtering results indicate that particular GCMs and ET methods drive the projection of wetter or drier future conditions much more than RCP trajectory; however the set of GCMs and ET methods that produce wetter or drier projections varies substantially by region. Results of this study indicate that, in addition to using an ensemble of GCMs and several RCP trajectories, a range of regionally-relevant ET estimation methods should be used to develop a robust range of future conditions for water resource planning under climate change.

HESSD
doi:10.5194/hess-2015-408

1 Introduction

Climate change will result in significant impacts on hydrologic processes. The 2014 Fifth Assessment Report (AR5) of the Intergovernmental Panel on Climate Change (IPCC) reported that climate change will significantly affect future precipitation (P), temperature (T) and evapotranspiration (ET) and these changes will affect the quantity and quality of water resources. The most recent report of the National Climate Assessment and Development Advisory Committee (NCADAC, 2013) indicated that the average annual temperature in the United States (US) has increased by 0.7 to 0.9 °C since record keeping began in 1895 and is expected to continue to rise (Georgakakos et al., 2014; Walsh et al., 2014). The NCADAC report also indicated that Coupled Model Intercomparison Project 5 (CMIP5) Global Climate Model (GCM) precipitation projections show a consistent increase in Alaska and the far north of the continental US and a consistent decrease in the far Southwest US, but that GCM projections are inconsistent in the precipitation transition zone of the US continent. The uncertainty in climate change projections makes actionable water resources planning difficult in many regions. In order to predict changes in the hydrologic cycle, and future water supply and demand, estimates of changes in P, T and ET must be evaluated on a regional basis, and the uncertainty of these estimates must be quantified (Ishak et al., 2010).

Previous research has evaluated existing and potential future spatiotemporal changes in P, T and ET for various regions around the globe (e.g. Chaouche et al., 2010; Chong-Hai and Ying, 2012; Johnson and Sharma, 2009; Kharin et al., 2013; Maurer and Hidalgo, 2008; Quintana Seguí et al., 2010; Sung et al., 2012; Thomas, 2000; Wang et al., 2013; Xu et al., 2006). It is well known that future GCM projections of temperature and precipitation vary significantly due to both the different radiative forcing assumptions of carbon dioxide scenarios (e.g. CMIP3 Special Report on Emissions Scenarios (SRES) and CMIP5 Representative Concentration Pathways (RCP trajectories)) and different GCM model physics (Hawkins and Sutton, 2009, 2010). Future ET projections have been shown to depend on ET estimation methods in ad-

HESSD
doi:10.5194/hess-2015-408

dition to GCMs. For example Kingston et al. (2009) used 5 GCMs from the CMIP3 climate projections and 6 different ET equations to estimate global ET and found that the choice of ET method contributes to different projections of the future state of water resources which varies by region. They found that the Hamon and Jensen–Haise ET estimates showed the greatest changes in both humid and arid regions while the Penman–Monteith and Priestley–Taylor estimates frequently showed smallest change. Similarly McAfee (2013) used three ET equations with 17 CMIP3 GCMs to evaluate the uncertainty of future global ET projections and found that the Hamon equation showed more significant and consistently positive trends in ET compared to the Preistly–Taylor and Penman methods.

Although these studies indicate that the choice of GCM, ET method and RCP trajectory all contribute to different regional projections of P, T, ET and thus future water availability, most studies have primarily focused on the uncertainties caused by GCMs and/or RCP trajectories. However hydrologic models developed to estimate future water availability as a result of projected climate change use many different types of ET estimation methods (Zhao et al., 2013). Because the choice of ET estimation method may be as important as the choice of GCM or RCP trajectory, better understanding of the contribution of each of these factors to the overall prediction uncertainty of future water availability is necessary (Taylor et al., 2013).

The objective of this research is to comprehensively evaluate the relative sensitivity of future P, ET and water availability (defined here as P–ET) projections to choice of GCM, ET method and RCP trajectory over the continental US. Variance-based global sensitivity analysis (Saltelli et al., 2010) and Monte Carlo Filtering (Rose et al., 1991) are used to quantify the uncertainty and important input factors controlling these projections. Global sensitivity analysis (GSA) quantifies the relative importance of multiple uncertain factors over the entire range of factor values, and thus is preferred over local, one factor at a time, sensitivity analysis (Homma and Saltelli, 1996; Saltelli, 1999). Monte Carlo Filtering can identify sets of model simulations and input factors that meet a specified criteria or threshold. Thus global sensitivity analysis and Monte Carlo Filtering offer an opportunity to gain insight into the sources of uncertainty, and drivers of particular types of wet/dry behavior, when estimating future water availability under projected climate change.

2 Methods

All retrospective and future climate variables were obtained from the CMIP5 archive (accessible for download at http://pcmdi9.llnl.gov/). The "historical" runs of CMIP5 were used for the retrospective period (1950–2005) and the same ensemble member runs (r1i1p1 ensemble) of CMIP5 were used for two future periods: future period 1 (2030–2060), and future period 2 (2070–2100). Data for three RCP trajectories, RCP2.6, RCP4.5 and RCP8.5 were included in the analyses. Taylor et al. (2012) describes an overview of CMIP5 and RCP trajectories and compares the differences between CMIP5 and CMIP3 model projections.

Data from the CMIP5 archive were used to calculate monthly mean P, ET, and P–ET for the retrospective and both future periods over each of the 9 US climate regions identified by the National Climatic Data Center (Karl and Koss, 1984, Fig. 1). Future changes in monthly mean P, ET, and P–ET were estimated by subtracting the monthly mean value for the retrospective period from the monthly mean value for future period 1 or future period 2, as appropriate (Baker and Huang, 2014).

Ten commonly used ET estimation methods (Hargreaves, Blaney–Criddle, Hamon, Kharrufa, Irmak-Rn, Irmak-Rs, Dalton, Meyer, Penman–Monteith and Priestley–Taylor) were used in this study. These ET estimation methods can be divided into potential ET (PET) estimated by the Priestley–Taylor and Kharrufa equations, and reference ET (RET) estimated by the other eight methods. The methods can be further classified into temperature-based ET equations (Hargreaves, Blaney–Criddle, Hamon, and Kharrufa), radiation-based ET equations (Irmak-Rn and Irmak-Rs), mass transfer-based ET equations (Dalton and Meyer), and combination ET equations (Penman–Monteith and Priestley–Taylor). These equations are well-described in many papers (e.g., Allen et al.,

HESSD
doi:10.5194/hess-2015-408

1998; Hargreaves and Allen, 2003; Irmak et al., 2003; Tabari, 2010; Tabari et al., 2013; Xu and Singh, 2001) and are summarized in Table 1 (hereafter precipitation is referred to as P, and PET and RET are both referred to as ET for convenience).

Variables directly used from the CMIP5 monthly model output included precipitation (pr), maximum and minimum temperature (tasmax and tasmin), radiation (rlds, rlus, rsds, and rsus), air pressure (psl and ps), and wind speed (sfcWind) (http://cmip-pcmdi.llnl.gov/cmip5/docs/standard_output.pdf). Other variables needed in the 10 evapotranspiration equations were calculated using the variables from CMIP5 monthly model output (for details see Table 1). Monthly output that included all the variables needed for the Penman–Monteith reference evapotranspiration method (the most data intensive method) was available for both the retrospective period, and for the RCP2.6, RCP 4.5, and RCP8.5 trajectories for the future periods, for 9 CMIP5 models. Table 2 lists the 9 models from the CMIP5 archive that were used in this study.

The sensitivity of changes in future P, ET and (P–ET) to the choice of GCM, ET estimation method, and RCP trajectory was evaluated using the variance-based GSA method of Saltelli et al. (2010). Given a model of the form $Y = f(X_1, X_2, \ldots X_k)$, with Y a scalar, the variance-based first order effect for a generic factor X_i can be written (Saltelli et al., 2010):

$$V_{X_i}\left(E_{X_{\sim i}}\left(Y|X_i\right)\right), \tag{1}$$

where X_i is the ith factor (in our case either GCM, ET method or RCP trajectory) and $X_{\sim i}$ is the vector of all factors except X_i. The expectation operator $E_{X_{\sim i}}(Y|X_i)$ indicates that the mean of Y is taken over all possible values of X except X_i (i.e. $X_{\sim i}$) while keeping X_i fixed. The variance, V_{X_i}, is then taken of this quantity over all possible values of X_i.

The first order sensitivity coefficient is expressed as:

$$S_i = \frac{V_{X_i}(E_{X_{\sim i}}(Y|X))}{V(Y)}. \tag{2}$$

HESSD
doi:10.5194/hess-2015-408

Where $V(Y)$ the total variance of Y over all X_i. S_i is a normalized index varying between 0 and 1, because $V_{X_i}(E_{X_{\sim i}}(Y|X_i))$ varies between 0 and $V(Y)$ according to the identity (Mood et al., 1974):

$$V_{X_i}\left(E_{X_{\sim i}}\left(Y|X_i\right)\right) + E_{X_i}\left(V_{X_{\sim i}}\left(Y|X_i\right)\right) = V\left(Y\right). \tag{3}$$

As indicated above $V_{X_i}(E_{X_{\sim i}}(Y|X_i))$ is the first order effect of X_i on the model output Y, while $E_{X_i}(V_{X_{\sim i}}(Y|X_i))$ is called the residual. The total effect index, including first order and higher order effects (i.e. interactions between factor X_i and other factors) of the factor X_i on the model output is calculated (Saltelli et al., 2010):

$$S_{T_i} = \frac{E_{X_{\sim i}}\left(V_{X_i}\left(Y|X_{\sim i}\right)\right)}{V\left(Y\right)} = 1 - \frac{V_{X_{\sim i}}\left(E_{X_i}\left(Y|X_{\sim i}\right)\right)}{V\left(Y\right)}. \tag{4}$$

The first order sensitivity of estimated future changes in mean monthly P, ET, and P–ET to choice of GCM, ET estimation method and RCP trajectory were calculated over the 9 US climate regions for each future period in order to evaluate the relative contributions of each of these factors on the uncertainty of future changes. A total of 270 simulations (9 GCMs × 10 evapotranspiration methods × 3 RCP trajectories) was used in the analysis. Sensitivity of projected changes in P were evaluated for both choice of GCM and choice of RCP trajectory. Sensitivity of projected changes in ET and P–ET were evaluated for choice of GCM, choice of ET estimation method, and choice of RCP trajectory.

For projected changes in water availability (P–ET) Monte Carlo filtering (Saltelli et al., 2008) was used to identify whether projected wetter or drier future conditions (i.e. larger or smaller water availability) could be attributed to specific GCMs, ET estimation methods, or RCP trajectories. For each future period the ensemble of 270 projections of change in water availability were categorized as either wet future condition (mean change in (P–ET) ≥ 0) or dry future condition (mean change in (P–ET) < 0). Next for each factor (X_i = GCM, ET method, RCP trajectory) the histograms of wet ($f_{\text{wet}}|X_i$) and dry ($f_{\text{dry}}|X_i$) future conditions over the range of possible values of that factor were estimated. To identify the factors that are most responsible for driving the model into projected wet or dry future conditions for each factor, X_i, the distributions ($f_{\text{wet}}|X_i$) and ($f_{\text{dry}}|X_i$) were tested for significant difference using the X^2 two sample test for categorical variables with $\alpha = 0.05$ (Rao and Scott, 1981). If for a given factor X_i the two distributions are significantly different, then X_i is a key factor in driving into either a wet or dry condition (Saltelli et al., 2008).

3 Results and discussion

Future P, ET and water availability projections include large uncertainties stemming from different sources. Figures 2 and 3 present maps of the mean change (Fig. 2) and the standard deviation of change (Fig. 3) in annual P (top chart), ET (middle) and water availability (P – potential or reference ET; bottom) over the continental US calculated over all GCMs, ET estimation methods, and RCP trajectories for future period 2 (2070–2100). Major portions of the West, Southwest and South show a mean decrease in annual precipitation, while the rest of the continental US shows a mean increase (Fig. 2a). Future annual ET shows a mean increase over retrospective annual ET over the entire US (Fig. 2b), with the largest increase in the South region. Following the patterns of P and ET, future annual water availability (P–ET) shows a significant mean decrease in the West, Southwest and South regions and a slight decline, or negligible change in most other regions (Fig. 2c). These mean changes in annual P, ET and P–ET are relatively small compared to the standard deviation of changes in annual P, ET, and P–ET (Fig. 3). Water availability in particular has a large standard deviation, resulting in coefficients of variation larger than one throughout the continental US. These figures clearly show that the uncertainty caused by different GCMs, ET methods, and RCP trajectories make actionable water resources planning based on climate change projections difficult.

Figure 4 shows the seasonal changes in the monthly mean and standard deviation of water availability (P–ET) over the nine US regions. Blue and red lines represent the changes in monthly mean water availability for future period 1 and future period 2, respectively and the error bars represent one standard deviation around each mean value. All regions of the continental US show drier conditions (negative mean changes) in the summer season (June–August). Southern regions (Southeast, South, Southwest and West) show drier conditions throughout the year, however northern portions of the US (i.e. the Northeast, Ohio Valley, Upper Midwest, Northern Rockies and Plains and Northwest) show wetter conditions (positive mean changes) in the winter season. The results are consistent with those reported by McAfee (2013) who used 3 ET methods (Hamon, Priestly–Taylor and Penman–Monteith) to estimate global changes in ET over the entire globe. As found by Baker and Huang (2014) for both CMIP3 and CMIP5 projections, mean ET is projected to be higher in future period 2 than in future period 1, and mean precipitation projections are approximately equivalent in future period 1 and future period 2. Thus the projected mean changes in water availability for future period 2 (red lines in Fig. 4) are larger in magnitude than the projected changes for future period 1 (blue lines). In all regions, and for both future periods, the one standard deviation error bars bracket zero mean change indicating large uncertainty in the projections throughout the year.

Figure 5 shows the first order sensitivity of change in P to GCM and RCP trajectory over the nine US climate regions for future periods 1 and 2. For projected changes in P, the choice of GCM is generally more important than choice of RCP trajectory for all regions and both future periods. This is consistent with results found by Gaetani and Mohino (2013) and Knutti and Sedláček (2012) who showed significant differences in precipitation predictions among CMIP5 models. It should be noted that these results do not indicate that the choice of RCP trajectory does not affect the change in precipitation, only that the choice of RCP trajectory is less influential than the choice of GCM. There are no consistent seasonal patterns of the first-order sensitivity coefficients for either GCM or RCP trajectory in either future period. However, during the spring months, the

HESSD
doi:10.5194/hess-2015-408

sensitivity of change in P to choice of RCP trajectory increases substantially in future 2 compared to future 1 in the Northeast, Ohio Valley, Upper Midwest, South, Southwest and West regions.

First order sensitivities of mean change in ET to GCM, ET method and RCP trajectory are shown in Fig. 6. This figure clearly shows that the choice of ET method is the most influential factor for projecting change in ET for both future periods, except for the month of March in the Northeast, Upper Midwest and Northern Rockies and Plains. High sensitivity of mean change in ET to GCM selection occurs in spring for several regions (Northeast, Upper Midwest and Northern Rockies and Plains), indicating a divergence of model predictions during this time. The influence of the RCP trajectory on ET increases in future period 2 over future period 1, with a concomitant decrease in the influence of both ET method and GCM. In future period 1 the GCM sensitivity coefficients are greater than the RCP trajectory sensitivity coefficients over most regions; however, in future period 2 the RCP sensitivity coefficients become more important. These results are consistent with those found by sKingston et al. (2009) who showed that projected increase in ET varied by more than 100 % between ET methods, and Schwalm et al. (2013) who found the choice of ET estimation method is sensitive and even more influential than the choice of model in predicting ET; however, neither of these studies looked at the influence of RCP trajectory on ET projections.

Burke and Brown (2008) evaluated uncertainties in the projection of future drought using several drought indices. They found that there are large uncertainties in regional changes in drought and changes in drought are dependent on both index definition and GCM ensemble members. Similarly, Fig. 7 shows that projected change in water availability depend strongly on both the choice of GCM and ET estimation method. In all regions except the Southeast projected change in water availability is most sensitive to ET estimation method in the warm season (May through October) and most sensitive to GCM in the cool season (December through March). For the Southeast region the sensitivity coefficients for GCM and ET method are quite similar throughout the year. The sensitivity coefficients for RCP trajectory are very low in future 1, but increase in future 2, becoming approximately equal to the GCM sensitivity coefficients in the summer season in future 2. These results are similar to results reported by Orlowsky and Seneviratne (2013) who found that the greenhouse gas emission scenario uncertainty is not as important as differences among GCMs or internal climate variability when predicting Standardized Precipitation Index (SPI) and soil moisture (SMA). However, they also found that uncertainty due to greenhouse gas emission scenario increased in later future periods. Taylor et al. (2013) showed the patterns of changes in future drought were similar between the A1B scenario in CMIP3 and the RCP2.6 trajectory in CMIP5, reinforcing our finding that the choice of RCP trajectory is less important than the choice of GCM and ET estimation method when estimating future water availability.

The results of the GSA show that the choice of ET method has important implications when making future ET projections and future water availability projections. Many hydrologic models use a single evapotranspiration method for simulation, which may substantially increase the uncertainty, and reduce the reliability of future projections. Figure 8 shows the change in annual mean water availability over all 9 GCMs for the RCP 4.5 trajectory in future period 1 (2030–2060) predicted by the ten different ET methods used in this study (a: Hargreaves, b: Blaney–Criddle, c: Hamon, d: Kharrufa, e: Irmak-Rn, f: Irmak-Rs, g: Dalton, h: Meyer, i: Penman–Monteith, j: Priestley–Taylor). This figure clearly shows that the changes in water availability for future period 1 are diverse and depend strongly on the choice of ET method. Except for the Hargreaves method (Fig. 8a) the temperature based methods (e.g. Blaney–Criddle (Fig. 8b), Hamon (Fig. 8c) and Kharrufa (Fig. 8d)) predict drier conditions over the continental US than the other methods. The mass transfer based methods (e.g. Dalton (Fig. 8g) and Meyer (Fig. 8h)) predict generally wetter conditions over most of the continental US compared to other methods. The combination methods (Penman Monteith (Fig. 8i) and Priestly Taylor (Fig. 8j) and the radiation based methods (Irmak-Rn (Fig. 8e) and Irmak-Rs (Fig. 8f)) generally fall between the mass transfer based and temperature based methods, with the combination methods producing slightly drier conditions. Although most methods predict similar spatial patterns of water availability over the continental

HESSD
doi:10.5194/hess-2015-408

US (generally drier conditions in the West, Southwest and South and generally wetter elsewhere), the Hamon method predicts a different pattern of water availability over the Southwest, South and Northern Rockies and Plains regions.

Monte Carlo filtering (Saltelli et al., 2008) was conducted to further investigate whether projected wetter or drier future conditions (i.e. larger or smaller annual mean water availability) could be attributed to specific GCMs, ET estimation methods, or RCP trajectories. Figure 9 shows the histograms for wet conditions and dry conditions in future 2 over the Southeast US by GCM, ET method and RCP trajectory for the example month of July. Figure 10 shows similar histograms for the Northern Rockies and Plains, a region with differing behavior from the Southeast US. Table 3 shows the P value results for the X^2 test for all months in both futures for the Southeast and Northern Rockies and Plains regions. P values greater than 0.05 (in bold in the tables) indicate the two histograms are not significantly different from each other. Tables 4–6 show the fraction of time that a particular GCM (Table 4), ET method (Table 5), or RCP trajectory (Table 6) projected drier future conditions in each of the 9 US climate regions for each month, with fractions higher than 0.5 (in bold in the tables).

Monte Carlo filtering results indicate that GCM and ET methods both produce statistically significant different wet condition and dry condition histograms in both the Southeast and Northern Rockies and Plains regions for almost all months in both future periods indicating particular GCMs and ET methods tend to systematically produce wet or dry conditions (Fig. 9 and 10, Table 3). Some GCMs (i.e. MIROC_ESM and BCC-CSM (Table 4)) and ET methods (i.e. Priestley–Taylor, Blaney–Criddle, and Kharrufa (Table 5)) predict dry conditions a majority of the time for all regions in both future periods. However the remaining GCMs and ET methods project both wetter or drier futures depending on the region and future period. Results in Tables 4 through 6 show that for the South, West and Southwest regions drier conditions are predicted a majority of the time in both future periods by all GCMs and RCP trajectories, and all ET methods except Hargreaves. For RCP trajectory, P values indicate the histograms are statistically significantly different in fewer cases than for either GCM or ET method for both future 1 and 2 (Table 3). These results are consistent with the first order sensitivity coefficients results that showed the RCP trajectory is not as important a factor as GCM or ET method in driving differences in future projections, but that the sensitivity to choice of RCP trajectory increases in future period 2.

4 Conclusions

Future changes in precipitation and evapotranspiration will lead to changes in the hydrologic cycle. Understanding and quantifying how these projected changes vary with choice of GCM, ET method and RCP trajectory is important for designing robust ensembles of scenarios to include in future water resources planning. This study assessed the future mean change in monthly precipitation, evapotranspiration and water availability (P–ET) projected by CMIP5 simulations over the continental US and analyzed the sensitivity of the projected changes to the choice of GCM, ET estimation method, and RCP trajectory. Nine GCMs, ten ET estimation methods, and three RCP trajectories were included in the analyses. Variance-based global sensitivity analysis (Saltelli et al., 2010) was conducted in order to determine the relative contributions of the choice of GCMs, ET estimation methods, and RCP trajectory to uncertainty in future prediction. Monte Carlo filtering was used to investigate whether particular GCMs, ET methods, and/or RCP scenarios consistently led to wet or dry future projections.

The CMIP5 results, when averaged over nine GCMs, ten ET methods, and three RCP trajectories, indicate that the West, Southwest, and South US are projected to experience a decrease in annual precipitation, while all other regions of the continental US are projected experience an increase in annual mean precipitation for both future periods 1 and 2. An increase in annual mean ET is predicted over the entire continental US for both future periods, with the largest increases in West, South and Southeast. Future water availability is projected to significantly decrease in the West, Southwest, and South regions of the continental US. A slight decline or negligible change is projected in most other regions. The standard deviations of projected changes in P, ET and

HESSD
doi:10.5194/hess-2015-408

P–ET are large compared to the mean changes, making actionable water resources planning based on these climate change projections difficult.

The global sensitivity analyses showed that projected changes in precipitation are more sensitive to the choice of GCM than the choice of RCP trajectory over the entire continental US for both future periods. However the choice of RCP trajectory becomes more important in future period 2. The most sensitive factor for the future ET projections is the choice of ET estimation method for all regions in both future periods. The first order sensitivity of projected change in future ET to choice of RCP trajectory increases in future period 2 compared to future 1, with a concomitant decrease in the first order sensitivity to the choice of GCM. For projected change in future water availability the choice of ET method constitutes the dominant source of uncertainty in warmer months (May through September) and the choice of GCM is the dominant source of uncertainty in the cooler months (November through March) over all regions except the Southeast where the sensitivity of GCM and ET method are roughly equal throughout the year. Sensitivity of change in future water availability to RCP trajectory is very small for future period 1, but increased in future period 2.

Monte Carlo filtering results indicated that both GCMs and ET methods produced statistically different histograms for wetter or drier future conditions (i.e. larger or smaller mean future water availability) for almost all months in both future periods. Two GCMs (MIROC_ESM and BCC-CSM) and three ET methods (Priestley–Taylor, Blaney–Criddle, and Kharrufa) predicted dry conditions a majority of the time for all regions in both future periods; however, the remaining GCMs and ET methods projected both wetter and drier futures depending on the region.

Results of this study indicate that when predicting the effects of future climate on water resources the choice of evapotranspiration method should be carefully evaluated. Rather than the typical practice of using a single ET method to drive a hydrologic model with future climate projections, an ensemble of ET methods should be used in addition to an ensemble of GCMs and a variety of RCP trajectories. The GSA methodology adopted here assumed that all the GCMs, ET methods and RCP trajectories used in

HESSD
doi:10.5194/hess-2015-408

this study were equally appropriate for use in all US regions (i.e the sensitivity coefficients were evaluated by equally weighting each GCM, ET method and RCP trajectory) which is likely not to be the case. When making future projections of potential climate change on water resources Reliability Ensemble Averaging (REA) (Giorgi and Mearns, 2002) or Bayesian-based indicator-weighting (Asefa and Adams, 2013; Tebaldi et al., 2005) could be used to weight the results of an ensemble of GCMs and ET methods based on how close the retrospective GCM-ET method predictions agree with past observations (bias criterion) and how well the future GCM-ET-RCP projections agree with other future GCM-ET-RCP predictions (convergence criterion).

This study assumed that ET methods that have been developed and parameterized based on vegetation response to current CO_2 levels and climatic conditions will be valid under future CO_2 levels and climatic conditions. Future research should explore the validity of this assumption by incorporating potential changes in plant transpiration (e.g. stomatal conductance) to changing CO_2 levels into the ET estimation methodologies.

Acknowledgements. This research was supported by Tampa Bay Water and the University of Florida Water Institute. We acknowledge the modeling groups participating in the Program for Climate Model Diagnosis and Inter-comparison (PCMDI) for their role in making the CMIP5 (Coupled Model Intercomparison Project) multi-model data set available.

References

Allen, R. G., Pereira, L. S., Raes, D., and Smith, M.: Crop evapotranspiration: guidelines fo computing crop water requirements, FAO Irrigation Drainage Paper 56, FAO, Rome, 300, D05109, 1998.

Asefa, T. and Adams, A.: Reducing bias-corrected precipitation projection uncertainties: a Bayesian-based indicator-weighting approach, Reg. Environ. Chang., 13, 111–120, doi:10.1007/s10113-013-0431-9, 2013.

Baker, N. C. and Huang, H. P.: A comparative study of precipitation and evaporation between CMIP3 and CMIP5 Climate Model Ensembles in semiarid regions, J. Climate, 27, 3731–3749, doi:10.1175/JCLI-D-13-00398.1, 2014.

Bentsen, M., Bethke, I., Debernard, J. B., Iversen, T., Kirkevåg, A., Seland, Ø., Drange, H., Roelandt, C., Seierstad, I. A., Hoose, C., and Kristjánsson, J. E.: The Norwegian Earth System Model, NorESM1-M – Part 1: Description and basic evaluation of the physical climate, Geosci. Model Dev., 6, 687–720, doi:10.5194/gmd-6-687-2013, 2013.

Block, K. and Mauritsen, T.: Forcing and feedback in the MPI-ESM-LR coupled model under abruptly quadrupled CO_2, J. Adv. Model. Earth Syst., 5, 676–691, doi:10.1002/jame.20041, 2013.

Burke, E. J. and Brown, S. J.: Evaluating uncertainties in the projection of future drought, J. Hydrometeorol., 9, 292–299, doi:10.1175/2007JHM929.1, 2008.

Chaouche, K., Neppel, L., Dieulin, C., Pujol, N., Ladouche, B., Martin, E., Salas, D., and Caballero, Y.: Analyses of precipitation, temperature and evapotranspiration in a French Mediterranean region in the context of climate change, Comptes Rendus Geosci., 342, 234–243, doi:10.1016/j.crte.2010.02.001, 2010.

Chong-Hai, X. and Ying, X.: The projection of temperature and precipitation over China under RCP scenarios using a CMIP5 multi-model ensemble, Atmos. Ocean. Sci., 5, 527–533, 2012.

Gaetani, M. and Mohino, E.: Decadal prediction of the sahelian precipitation in CMIP5 simulations, J. Climate, 26, 7708–7719, doi:10.1175/JCLI-D-12-00635.1, 2013.

Georgakakos, A., Fleming, P., Dettinger, M., Peters-Lidard, C., Richmond, T., Reckhow, K., White, K., and Yates, D.: Ch. 3: Water resources, in: Climate Change Impacts in the United States: The Third National Climate Assessment, edited by: Melillo, J. M., Richmond, T. C., and Yohe, G. W., US Global Change Research Program, 69–112, doi:10.7930/J0G44N6T, 2014.

Giorgi, F. and Mearns, L.: Calculation of average, uncertainty range, and reliability of regional climate changes from AOGCM simulations via the "reliability ensemble averaging"(REA) method, J. Climate, 15, 1141–1158, doi:10.1175/1520-0442(2002)015<1141:COAURA>2.0.CO;2, 2002.

Guo, H., Golaz, J.-C., Donner, L. J., Ginoux, P., and Hemler, R. S.: Multivariate probability density functions with dynamics in the GFDL Atmospheric General Circulation Model: global tests, J. Climate, 27, 2087–2108, doi:10.1175/JCLI-D-13-00347.1, 2014.

Hargreaves, G. H. and Allen, R. G.: History and evaluation of Hargreaves evapotranspiration equation, J. Irrig. Drain. Eng., 129, 53–63, doi:10.1061/(ASCE)0733-9437(2003)129:1(53), 2003.

HESSD

doi:10.5194/hess-2015-408

Sensitivity of future water availability projections to Global Climate Model

S. Chang et al.

Hawkins, E. and Sutton, R.: The potential to narrow uncertainty in regional climate predictions, B. Am. Meteorol. Soc., 90, 1095–1107, doi:10.1175/2009BAMS2607.1, 2009.
Hawkins, E. and Sutton, R.: The potential to narrow uncertainty in projections of regional precipitation change, Clim. Dynam., 37, 407–418, doi:10.1007/s00382-010-0810-6, 2010.
Homma, T. and Saltelli, A.: Importance measures in global sensitivity analysis of nonlinear models, Reliab. Eng. Syst. Saf., 52, 1–17, doi:10.1016/0951-8320(96)00002-6, 1996.
Irmak, S., Irmak, A., Allen, R. G., and Jones, J. W.: Solar and Net Radiation-Based Equations to Estimate Reference Evapotranspiration in Humid Climates, J. Irrig. Drain. Eng., 129, 336–347, doi:10.1061/(ASCE)0733-9437(2003)129:5(336), 2003.
Ishak, A. M., Bray, M., Remesan, R., and Han, D.: Estimating reference evapotranspiration using numerical weather modelling, Hydrol. Process., 24, 3490–3509, doi:10.1002/hyp.7770, 2010.
Ji, D., Wang, L., Feng, J., Wu, Q., Cheng, H., Zhang, Q., Yang, J., Dong, W., Dai, Y., Gong, D., Zhang, R.-H., Wang, X., Liu, J., Moore, J. C., Chen, D., and Zhou, M.: Description and basic evaluation of BNU-ESM version 1, Geosci. Model Dev. Discuss., 7, 1601–1647, doi:10.5194/gmdd-7-1601-2014, 2014.
Johnson, F. and Sharma, A.: Measurement of GCM skill in predicting variables relevant for hydroclimatological assessments, J. Climate, 22, 4373–4382, doi:10.1175/2009JCLI2681.1, 2009.
Karl, T. R. and Koss, W. J.: Historical Climatology Series 4-3: Regional and National Monthly, Seasonal, and Annual Temperature Weighted by Area, 1895–1983, available at: http://www.ncdc.noaa.gov/monitoring-references/maps/us-climate-regions.php (last access: 4 January 2015), 1984.
Kharin, V. V., Zwiers, F. W., Zhang, X., and Wehner, M.: Changes in temperature and precipitation extremes in the CMIP5 ensemble, Clim. Change, 119, 345–357, doi:10.1007/s10584-013-0705-8, 2013.
Kingston, D. G., Todd, M. C., Taylor, R. G., Thompson, J. R., and Arnell, N. W.: Uncertainty in the estimation of potential evapotranspiration under climate change, Geophys. Res. Lett., 36, L20403, doi:10.1029/2009GL040267, 2009.
Knutti, R. and Sedláček, J.: Robustness and uncertainties in the new CMIP5 climate model projections, Nat. Clim. Chang., 3, 369–373, doi:10.1038/nclimate1716, 2012.

HESSD
doi:10.5194/hess-2015-408

Sensitivity of future water availability projections to Global Climate Model

S. Chang et al.

Maurer, E. P. and Hidalgo, H. G.: Utility of daily vs. monthly large-scale climate data: an intercomparison of two statistical downscaling methods, Hydrol. Earth Syst. Sci., 12, 551–563, doi:10.5194/hess-12-551-2008, 2008.

McAfee, S. A.: Methodological differences in projected potential evapotranspiration, Clim. Change, 120, 915–930, doi:10.1007/s10584-013-0864-7, 2013.

Mood, A. M., Graybill, F. A., and Boes, D. C.: Introduction to Theory of Statistics, McGraw-Hill, Inc., 129–167, 1974.

Orlowsky, B. and Seneviratne, S. I.: Elusive drought: uncertainty in observed trends and short- and long-term CMIP5 projections, Hydrol. Earth Syst. Sci., 17, 1765–1781, doi:10.5194/hess-17-1765-2013, 2013.

Quintana Seguí, P., Ribes, A., Martin, E., Habets, F., and Boé, J.: Comparison of three downscaling methods in simulating the impact of climate change on the hydrology of Mediterranean basins, J. Hydrol., 383, 111–124, doi:10.1016/j.jhydrol.2009.09.050, 2010.

Rao, J. N. K. and Scott, A. J.: The analysis of categorical data from complex sample survey: chi-squared tests for goodness of fit and independence in two-way tables, J. Am. Stat. Assoc., 76, 221–230, 1981.

Rose, K. A, Smith, E. P., Gardner, R. H., Brenkert, A. L., and Bartell, S. M.: Parameter sensitivities, monte carlo filtering, and model forecasting under uncertainty, J. Forecast., 10, 117–133, doi:10.1002/for.3980100108, 1991.

Rotstayn, L. D., Jeffrey, S. J., Collier, M. A., Dravitzki, S. M., Hirst, A. C., Syktus, J. I., and Wong, K. K.: Aerosol- and greenhouse gas-induced changes in summer rainfall and circulation in the Australasian region: a study using single-forcing climate simulations, Atmos. Chem. Phys., 12, 6377–6404, doi:10.5194/acp-12-6377-2012, 2012.

Saltelli, A.: Sensitivity analysis: could better methods be used?, J. Geophys. Res., 104, 3789, doi:10.1029/1998JD100042, 1999.

Saltelli, A., Ratto, M., Andres, T., Campolongo, F., Cariboni, J., Gatelli, D., Saisana, M., and Tarantola, S.: Global Sensitivity Analysis: the Primer, John Wiley & Sons, Inc., 155–163, 2008.

Saltelli, A., Annoni, P., Azzini, I., Campolongo, F., Ratto, M., and Tarantola, S.: Variance based sensitivity analysis of model output. Design and estimator for the total sensitivity index, Comput. Phys. Commun., 181, 259–270, doi:10.1016/j.cpc.2009.09.018, 2010.

Schwalm, C. R., Huntinzger, D. N., Michalak, A. M., Fisher, J. B., Kimball, J. S., Mueller, B., Zhang, K., and Zhang, Y.: Sensitivity of inferred climate model skill to evaluation de-

cisions: a case study using CMIP5 evapotranspiration, Environ. Res. Lett., 8, 024028, doi:10.1088/1748-9326/8/2/024028, 2013.
Sung, J. H., Kang, H.-S., Park, S., Cho, C., Bae, D. H., and Kim, Y.-O.: Projection of extreme precipitation at the end of 21st century over South Korea based on Representative Concentration Pathways (RCP), Atmosphere (Basel), 22, 221–231, doi:10.14191/Atmos.2012.22.2.221, 2012.
Tabari, H.: Evaluation of reference crop evapotranspiration equations in various climates, Water Resour. Manag., 24, 2311–2337, doi:10.1007/s11269-009-9553-8, 2010.
Tabari, H., Grismer, M. E., and Trajkovic, S.: Comparative analysis of 31 reference evapotranspiration methods under humid conditions, Irrig. Sci., 31, 107–117, doi:10.1007/s00271-011-0295-z, 2013.
Taylor, I. H., Burke, E., McColl, L., Falloon, P. D., Harris, G. R., and McNeall, D.: The impact of climate mitigation on projections of future drought, Hydrol. Earth Syst. Sci., 17, 2339–2358, doi:10.5194/hess-17-2339-2013, 2013.
Taylor, K. E., Stouffer, R. J., and Meehl, G. A.: An overview of CMIP5 and the experiment design, B. Am. Meteorol. Soc., 93, 485–498, doi:10.1175/BAMS-D-11-00094.1, 2012.
Tebaldi, C., Smith, R. L., Nychka, D., and Mearns, L. O.: Quantifying uncertainty in projections of regional climate change: a bayesian approach to the analysis of multimodel ensembles, J. Climate, 18, 1524–1540, doi:10.1175/JCLI3363.1, 2005.
Thomas, A.: Spatial and temporal characteristics of potential evapotranspiration trends over China, Int. J. Climatol., 20, 381–396, doi:10.1002/(SICI)1097-0088(20000330)20:4<381::AID-JOC477>3.0.CO;2-K, 2000.
Walsh, J., Wuebbles, D., Hayhoe, K., Kossin, J., Stephens, G., Thorne, P., Vose, R., Wehner, M., Willis, J., Anderson, D., Doney, S., Feely, R., Hennon, P., Kharin, V., Knutson, T., Landerer, F., Lenton, T., Kennedy, J., and Somerville, R.: Ch. 2: Our changing climate, in: Climate Change Impacts in the United States: The Third National Climate Assessment, Melillo, J. M., Richmond, T. C., and Yohe, G. W., US Global Change Research Program, 19–67, doi:10.7930/J0KW5CXT, 2014.
Wang, W., Xing, W., Shao, Q., Yu, Z., Peng, S., Yang, T., Yong, B., Taylor, J., and Singh, V. P.: Changes in reference evapotranspiration across the Tibetan Plateau: observations and future projections based on statistical downscaling, J. Geophys. Res. Atmos., 118, 4049–4068, doi:10.1002/jgrd.50393, 2013.

Watanabe, S., Hajima, T., Sudo, K., Nagashima, T., Takemura, T., Okajima, H., Nozawa, T., Kawase, H., Abe, M., Yokohata, T., Ise, T., Sato, H., Kato, E., Takata, K., Emori, S., and Kawamiya, M.: MIROC-ESM: model description and basic results of CMIP5-20c3m experiments, Geosci. Model Dev. Discuss., 4, 1063–1128, doi:10.5194/gmdd-4-1063-2011, 2011.

Xiao-Ge, X., Tong-Wen, W., Jiang-Long, L., Zai-Zhi, W., Wei-Ping, L., and Fang-Hua, W.: How well does BCC_CSM1.1 reproduce the 20th century climate change over China?, Atmos. Ocean. Sci. Lett., 6, 21–26, 2013.

Xu, C. and Singh, V. P.: Evaluation and generalization of temperature-based methods for calculating evaporation, Hydrol. Process., 15, 305–319, doi:10.1002/hyp.119, 2001.

Xu, C. and Singh, V.: Cross comparison of empirical equations for calculating potential evapotranspiration with data from Switzerland, Water Resour. Manag., 16, 197–219, doi:10.1023/A:1020282515975, 2002.

Xu, C., Gong, L., Jiang, T., Chen, D., and Singh, V. P.: Analysis of spatial distribution and temporal trend of reference evapotranspiration and pan evaporation in Changjiang (Yangtze River) catchment, J. Hydrol., 327, 81–93, doi:10.1016/j.jhydrol.2005.11.029, 2006.

Yukimoto, S., Adachi, Y., Hosaka, M., Sakami, T., Yoshimura, H., Hirabara, M., Tanaka, T. Y., Shindo, E., Tsujino, H., Deushi, M., Mizuta, R., Yabu, S., Obata, A., Nakano, H., Koshiro, T., Ose, T., and Kitoh, A.: A new global climate model of the meteorological research institute: MRI-CGCM3 – model description and basic performance, J. Meteorol. Soc. Japan, 90A, 23–64, doi:10.2151/jmsj.2012-A02, 2012.

Zhao, L., Xia, J., Xu, C., Wang, Z., Sobkowiak, L., and Long, C.: Evapotranspiration estimation methods in hydrological models, J. Geogr. Sci., 23, 359–369, doi:10.1007/s11442-013-1015-9, 2013.

HESSD
doi:10.5194/hess-2015-408

Table 1. Description of evapotranspiration estimation methods used in this study (ET_0: reference evapotranspiration, and PET: potential evapotranspiration).

Methods	Equations[1]	Reference
(a) Hargreaves	$ET_0 = 0.0135 K_T S_0 (T + 17.8)\sqrt{\delta_T}$	Hargreaves and Allen (2003)
(b) Blaney–Criddle	$ET_0 = p(0.46T + 8.13)$	Xu and Singh (2002)
(c) Hamon	$ET_0 = 0.55\delta_T^2 P_t$	Xu and Singh (2002)
(d) Kharrufa	$PET = 0.34pT^{1.3}$	Xu and Singh (2002)
(e) Irmak-Rn	$ET_0 = 0.486 + 0.289R_n + 0.023T$	Irmak et al. (2003)
(f) Irmak-Rs	$ET_0 = -0.611 + 0.149R_s + 0.079T$	Irmak et al. (2003)
(g) Dalton	$ET_0 = (0.3648 + 0.07223u)(e_s - e_a)$	Tabari et al. (2013)
(h) Meyer	$ET_0 = (0.375 + 0.05026u)(e_s - e_a)$	Tabari et al. (2013)
(i) Penman–Monteith	$ET_0 = \frac{0.408\Delta(R_n - G) + \gamma\frac{900}{T+273}u_2(e_s - e_a)}{\Delta + \gamma(1 + 0.34u_2)}$	Allen et al. (1998)
(j) Priestley–Taylor	$PET = \alpha\frac{\Delta}{\Delta+\gamma}\frac{(R_n - G)}{\lambda}$	Allen et al. (1998)

[1] Variables (estimated from CMIP5 outputs): G: soil heat flux (assumed 0); γ: psychrometric constant; T: average temperature; u_2: wind speed at 2 m surface; e_s: saturated vapor pressure; e_a: actual vapor pressure; Δ: slope vapor pressure; K_T: Hargreaves–Samani coefficient; S_0: extraterrestrial radiation (estimated by Julian date); δ_T: difference between maximum and minimum temperature, p: percentage of total daytime hours (Estimated by Julian date); R_n: net radiation; R_s: solar radiation; P_t: saturated water vapor density; u: wind speed.

HESSD
doi:10.5194/hess-2015-408

Table 2. Description of the CMIP5 models used in this study.

Model	Institute (country)	Resolutions	Calendar	Reference
(1) BNU-ESM	College of Global Change and Earth System Science, Beijing Normal University (China)	2.8° lat × 2.8° lon	No leap	Ji et al. (2014)
(2) CSIRO-MK3-6-0	University of New South Wales (Australia)	1.87° lat × 1.87° lon	No leap	Rotstayn et al. (2012)
(3) GFDL-CM3	NOAA/Geophysical Fluid Dynamics Laboratory (USA)	2.0° lat × 2.5° lon	No leap	Guo et al. (2014)
(4) GFDL-ESM2G	NOAA/Geophysical Fluid Dynamics Laboratory (USA)	2.0° lat × 2.5° lon	No leap	Taylor et al. (2012)
(5) MIROC-ESM	Atmosphere and Ocean Research Institute, National Institute for Environmental Studies, and Japan Agency for Marine-Earth Science and Technology (Japan)	2.8° lat × 2.8° lon	Leap year	Watanabe et al. (2011)
(6) MPI-ESM-LR	Max Planck Institute for Meteorology (Germany)	1.87° lat × 1.87° lon	Leap year	Block and Mauritsen (2013)
(7) MRI-CGCM3	Meteorological Research Institute (Japan)	1.12° lat × 1.12° lon	Leap year	Yukimoto et al. (2012)
(8) NorESM1-M	Norwegian Climate Centre (Norway)	1.9° lat × 2.5° lon	No leap	Bentsen et al. (2013)
(9) BCC-CSM1.1	Beijing Climate Center (China)	2.8° lat × 2.8° lon	No leap	Xiao-Ge et al. (2013)

HESSD
doi:10.5194/hess-2015-408

Table 3. P values of Chi-square two sample test for difference among wet condition vs. dry condition pdfs Southeast US (SE US) and Northern Rockies and Plains (NRP; West North Central) US (bold values indicate pdfs are not statistically significantly different at $p = 0.05$).

Month		Future 1			Future 2		
		GCM	ET	RCP	GCM	ET	RCP
SE US	1	0.0000	**0.0689**	**0.3701**	0.0000	**0.1823**	**0.1853**
	2	0.0000	**0.0889**	**0.4434**	0.0000	0.0269	0.0000
	3	0.0000	0.0365	0.0306	0.0000	0.0000	**0.1339**
	4	0.0000	0.0000	**0.6602**	0.0000	0.0000	0.0001
	5	0.0000	0.0000	**0.3223**	0.0000	0.0000	0.0041
	6	0.0000	0.0000	**0.0809**	0.0000	0.0000	0.0006
	7	0.0000	0.0000	**0.2855**	0.0000	0.0000	**0.0749**
	8	0.0000	0.0000	**0.2805**	0.0000	0.0000	0.0074
	9	0.0000	0.0000	**0.8646**	0.0000	0.0000	0.0044
	10	0.0000	0.0000	0.0000	0.0000	0.0000	0.0001
	11	0.0000	0.0001	0.0000	0.0000	0.0001	**0.2003**
	12	0.0000	0.0117	**0.3083**	0.0000	0.0000	0.0000
NRP	1	0.0000	0.0000	**0.1931**	0.0000	0.0000	0.0000
	2	0.0000	0.0000	0.0010	0.0000	0.0000	**0.7617**
	3	0.0000	0.0000	**0.0538**	0.0000	0.0000	**0.0769**
	4	0.0000	0.0000	**0.7882**	0.0002	0.0000	**0.8925**
	5	0.0000	0.0000	**0.4047**	0.0000	0.0000	**0.1103**
	6	0.0000	0.0000	**0.3839**	0.0000	0.0000	0.0000
	7	0.0000	0.0000	**0.5321**	0.0001	0.0008	0.0000
	8	0.0000	0.0001	**0.1544**	0.0000	**0.0686**	0.0000
	9	0.0000	0.0000	**0.4242**	0.0000	0.0000	**0.2002**
	10	0.0000	0.0000	**0.6688**	0.0000	0.0213	0.0001
	11	0.0000	0.0000	**0.1334**	0.0000	0.0000	**0.1948**
	12	0.0000	0.0000	**0.7617**	0.0000	0.0000	**0.6561**

HESSD
doi:10.5194/hess-2015-408

Table 4. The fraction of future dry conditions over all months by GCM (Future period 1 and 2).

	GCM	SE	South	West	NR	NE	NW	UM	SW	Ohio
Future period 1 – Dry condition	BNU_ESM	**0.575**	**0.589**	**0.511**	0.367	0.436	0.322	0.467	0.453	0.492
	CSIRO_mk3_6_0	0.489	**0.689**	**0.639**	**0.547**	0.297	**0.519**	0.381	**0.653**	0.481
	GFDL_CM3	0.414	**0.608**	**0.686**	0.419	0.403	**0.525**	0.383	**0.647**	0.425
	GFDL_ESM2G	**0.731**	**0.900**	**0.758**	0.453	0.486	0.486	0.397	**0.828**	**0.617**
	MIROC_ESM	**0.631**	**0.594**	**0.822**	**0.625**	**0.636**	**0.708**	**0.686**	**0.658**	**0.611**
	MPI_ESM_LR	0.375	**0.747**	**0.694**	**0.542**	**0.597**	**0.611**	**0.558**	**0.756**	**0.575**
	MRI_CGCM3	0.494	**0.592**	**0.639**	0.400	**0.544**	**0.553**	0.350	**0.547**	**0.506**
	NorESM1_M	0.492	**0.764**	**0.778**	0.475	0.400	**0.611**	0.475	**0.753**	**0.508**
	BCC_CSM	**0.728**	**0.739**	**0.828**	**0.642**	**0.603**	**0.614**	**0.564**	**0.822**	**0.656**
Future period 2 – Dry condition	BNU_ESM	**0.608**	**0.775**	**0.597**	0.400	**0.522**	0.461	0.478	**0.522**	**0.572**
	CSIRO_mk3_6_0	0.367	**0.667**	**0.583**	**0.528**	0.225	**0.528**	0.433	**0.633**	0.461
	GFDL_CM3	0.467	**0.767**	**0.789**	0.461	**0.514**	**0.542**	**0.508**	**0.794**	0.469
	GFDL_ESM2G	**0.722**	**0.831**	**0.694**	0.478	**0.519**	**0.525**	0.397	**0.672**	**0.581**
	MIROC_ESM	**0.672**	**0.686**	**0.897**	**0.742**	**0.731**	**0.728**	**0.700**	**0.739**	**0.664**
	MPI_ESM_LR	0.442	**0.800**	**0.778**	**0.519**	**0.542**	**0.639**	0.450	**0.800**	0.450
	MRI_CGCM3	**0.508**	**0.703**	**0.581**	0.422	0.481	**0.528**	0.439	**0.517**	**0.556**
	NorESM1_M	**0.594**	**0.808**	**0.722**	**0.500**	0.461	**0.550**	0.481	**0.731**	**0.594**
	BCC_CSM	**0.628**	**0.697**	**0.875**	**0.708**	**0.567**	**0.708**	**0.556**	**0.825**	**0.603**

HESSD
doi:10.5194/hess-2015-408

Sensitivity of future water availability projections to Global Climate Model

S. Chang et al.

Table 5. The fraction of future dry condition over all months by ET estimation method and region (Future period 1 and 2).

	ET	SE	South	West	NR	NE	NW	UM	SW	Ohio
Future period 1 – Dry condition	Hargreaves	0.302	0.426	**0.559**	0.333	0.309	0.466	0.321	0.485	0.324
	Blaney_Criddle	**0.738**	**0.880**	**0.898**	**0.840**	**0.738**	**0.762**	**0.784**	**0.904**	**0.769**
	Hamon	**0.633**	**0.818**	**0.667**	**0.531**	0.494	0.497	0.457	**0.713**	**0.549**
	Kharrufa	**0.883**	**0.957**	**0.889**	**0.636**	**0.667**	**0.698**	**0.636**	**0.886**	**0.738**
	Irmak_Rn	**0.522**	**0.673**	**0.694**	0.491	**0.512**	**0.556**	0.494	**0.679**	**0.580**
	Irmak_Rs	**0.525**	**0.722**	**0.731**	0.463	0.485	**0.546**	0.460	**0.679**	**0.556**
	Dalton	0.364	**0.503**	**0.583**	0.340	0.343	0.426	0.296	**0.509**	0.380
	Meyer	0.367	**0.531**	**0.596**	0.346	0.324	0.435	0.290	**0.512**	0.367
	PM	**0.534**	**0.685**	**0.694**	0.472	0.469	**0.525**	0.481	**0.676**	**0.540**
	PT	**0.608**	**0.719**	**0.750**	**0.515**	**0.552**	**0.590**	**0.515**	**0.753**	**0.608**
Future period 2 – Dry condition	Hargreaves	0.352	**0.506**	**0.605**	0.420	0.355	0.491	0.380	**0.537**	0.361
	Blaney_Criddle	**0.765**	**0.907**	**0.880**	**0.877**	**0.769**	**0.818**	**0.830**	**0.901**	**0.806**
	Hamon	**0.633**	**0.861**	**0.679**	**0.552**	0.491	**0.528**	0.460	**0.719**	**0.574**
	Kharrufa	**0.883**	**0.954**	**0.898**	**0.704**	**0.713**	**0.728**	**0.682**	**0.883**	**0.784**
	Irmak_Rn	**0.515**	**0.738**	**0.710**	0.494	0.491	**0.574**	**0.503**	**0.685**	**0.543**
	Irmak_Rs	**0.534**	**0.796**	**0.753**	0.485	0.497	**0.562**	0.478	**0.719**	**0.562**
	Dalton	0.349	**0.596**	**0.620**	0.389	0.358	0.475	0.315	**0.540**	0.373
	Meyer	0.352	**0.596**	**0.630**	0.383	0.349	0.488	0.309	**0.546**	0.361
	PM	**0.543**	**0.744**	**0.701**	0.475	0.485	**0.531**	0.463	**0.679**	**0.528**
	PT	**0.639**	**0.784**	**0.765**	**0.509**	**0.562**	**0.593**	**0.515**	**0.716**	**0.608**

HESSD
doi:10.5194/hess-2015-408

Table 6. The fraction of future dry condition over all months by RCP trajectory and region (Future period 1 and 2).

	RCP	SE	South	West	NR	NE	NW	UM	SW	Ohio
Future period 1 – Dry condition	2.6	**0.551**	**0.657**	**0.665**	**0.507**	**0.502**	**0.543**	0.495	**0.644**	**0.553**
	4.5	**0.553**	**0.698**	**0.739**	**0.515**	0.475	**0.554**	0.482	**0.731**	**0.556**
	8.5	**0.539**	**0.719**	**0.715**	0.468	0.491	**0.554**	0.443	**0.665**	**0.515**
Future period 2 – Dry condition	2.6	**0.516**	**0.649**	**0.657**	0.486	**0.524**	**0.515**	0.465	**0.617**	**0.545**
	4.5	0.490	**0.731**	**0.712**	**0.510**	0.476	**0.584**	0.494	**0.658**	**0.528**
	8.5	**0.664**	**0.864**	**0.803**	**0.590**	**0.520**	**0.637**	**0.521**	**0.803**	**0.577**

HESSD
doi:10.5194/hess-2015-408

Sensitivity of future water availability projections to Global Climate Model

S. Chang et al.

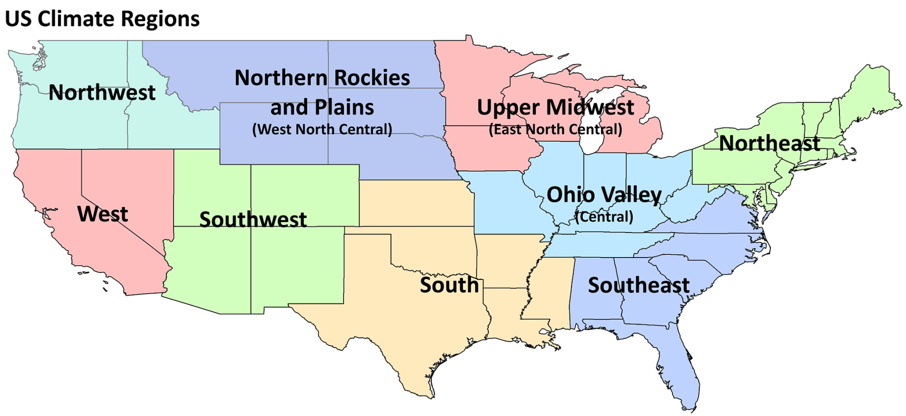

Figure 1. US climate regions identified by National Climate Data Center (Adapted from Karl and Koss, 1984, https://www.ncdc.noaa.gov/monitoring-references/maps/us-climate-regions.php).

HESSD
doi:10.5194/hess-2015-408

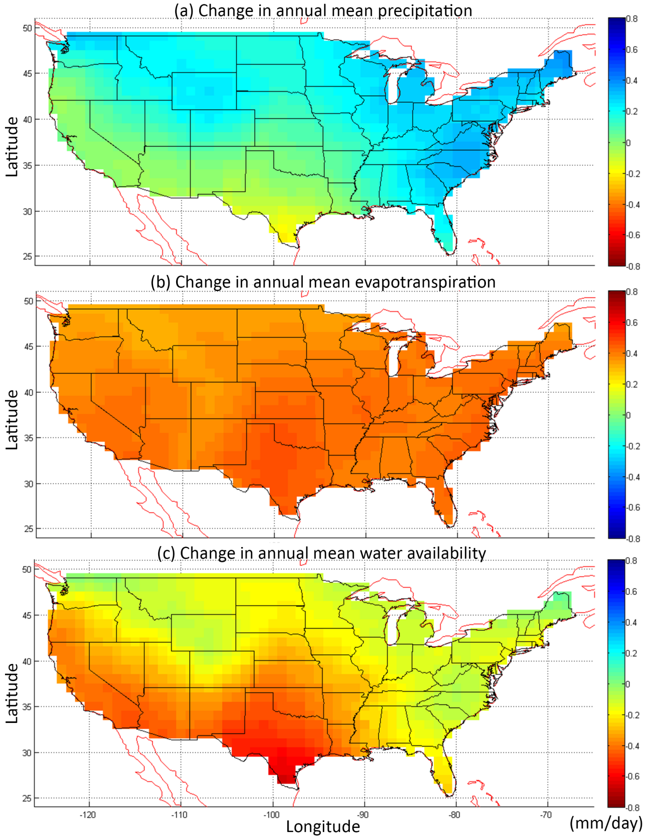

Figure 2. The change in the annual mean **(a)** P, **(b)** ET, and **(c)** P–ET over US. All units are $\mathrm{mm\,day^{-1}}$ and the change is defined as the mean of 2070–2100 minus that of 1950–2005. These changes are averaged over all GCMs, ET estimation methods, and RCP trajectories.

HESSD
doi:10.5194/hess-2015-408

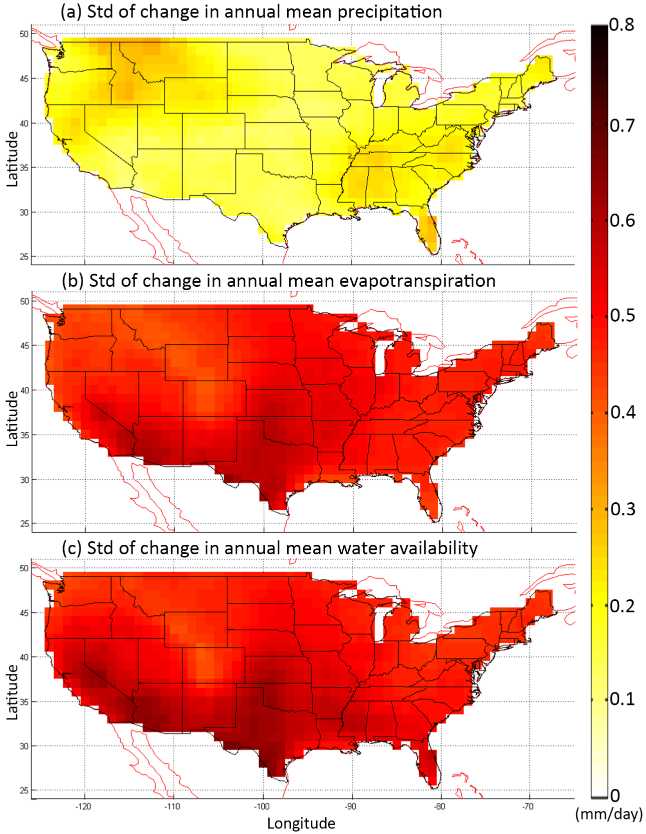

Figure 3. The standard deviation of the change in the annual mean **(a)** P, **(b)** ET, and **(c)** P–ET over US. All units are mm day^{-1} and the change is defined as the average of 2070–2100 minus that of 1950–2005. The standard deviations are estimated over all GCMs, ET estimation methods, and RCP trajectories.

HESSD
doi:10.5194/hess-2015-408

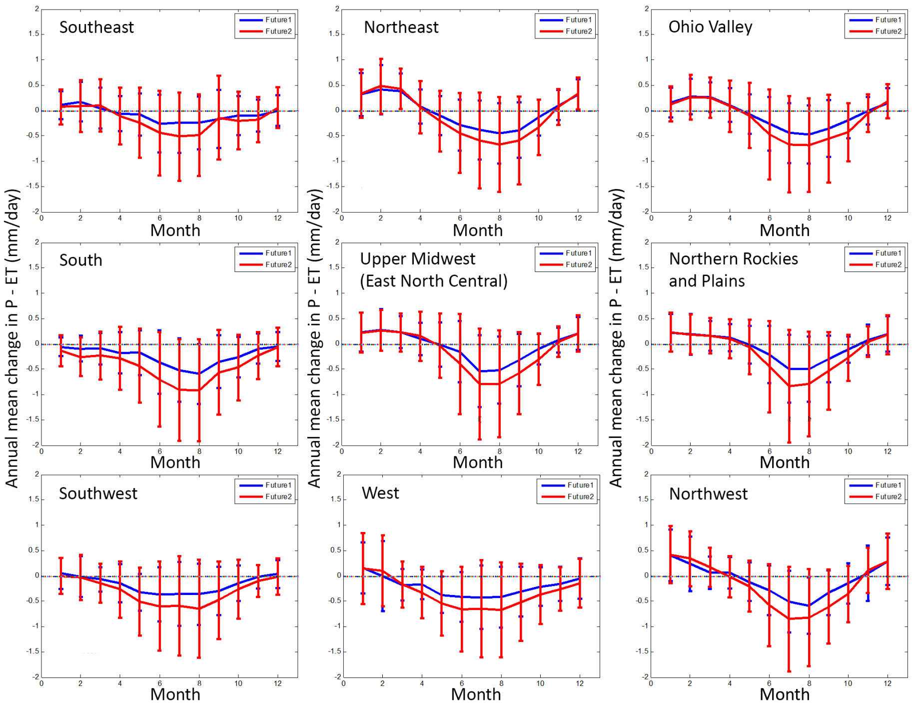

Figure 4. The change of monthly mean water availability (P–RET/PET) over 9 different regions. Blue lines represent future 1 period (2030–2060), and red lines represent future 2 period (2070–2100). Error bars represent one standard deviation of each values. The change is defined as the mean of future periods minus that of retrospective period (1950–2005).

HESSD
doi:10.5194/hess-2015-408

HESSD
doi:10.5194/hess-2015-408

Sensitivity of future water availability projections to Global Climate Model

S. Chang et al.

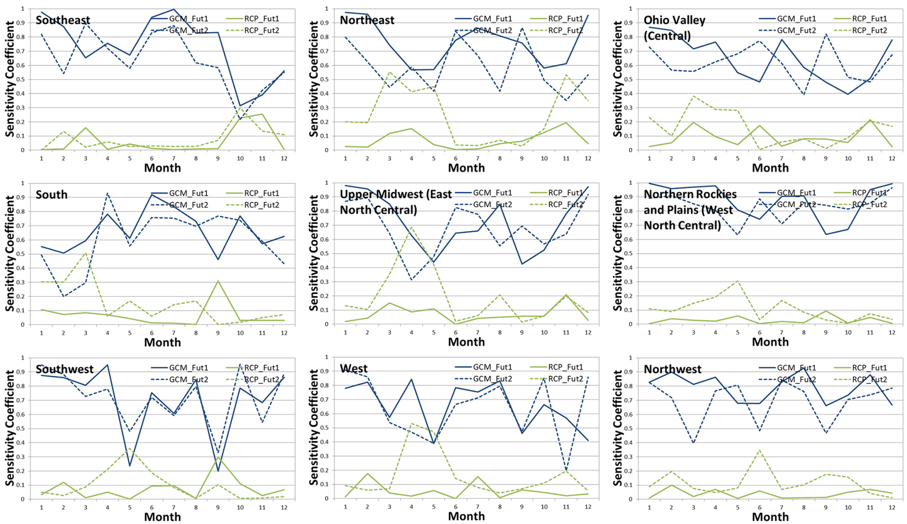

Figure 5. First order sensitivity analysis results of change in precipitation. Solid lines represent the future period 1 (2030–2060) and dotted lines represent the future period 2 (2070–2100). Blue lines represent the first order effect of GCMs and green lines represent the first order effect of RCPs.

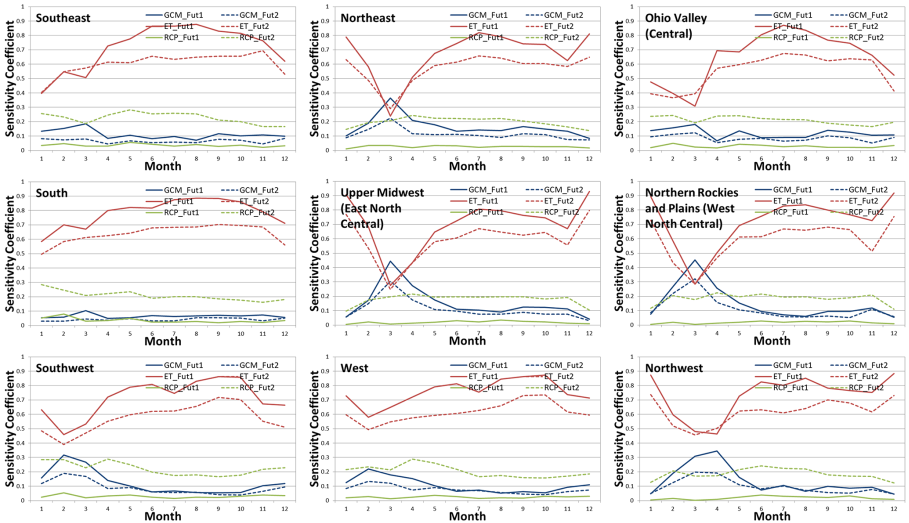

Figure 6. First order sensitivity analysis results of change in evapotranspiration. Solid lines represent the future period 1 (2030–2060) and dotted lines represent the future period 2 (2070–2100). Blue lines represent the first order effect of GCMs, red lines represent the first order effect of ET estimation methods and green lines represent the first order effect of RCPs.

HESSD
doi:10.5194/hess-2015-408

Sensitivity of future water availability projections to Global Climate Model

S. Chang et al.

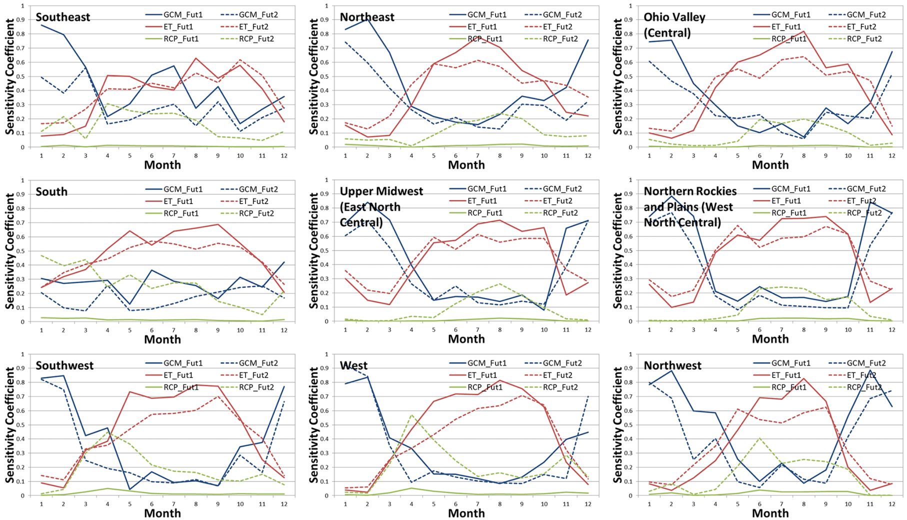

Figure 7. First order sensitivity analysis results of change in P–ET. Solid lines represent the future period 1 (2030–2060) and dotted lines represent the future period 2 (2070–2100). Blue lines represent the first order effect of GCMs, red lines represent the first order effect of ET estimation methods and green lines represent the first order effect of RCPs.

HESSD

doi:10.5194/hess-2015-408

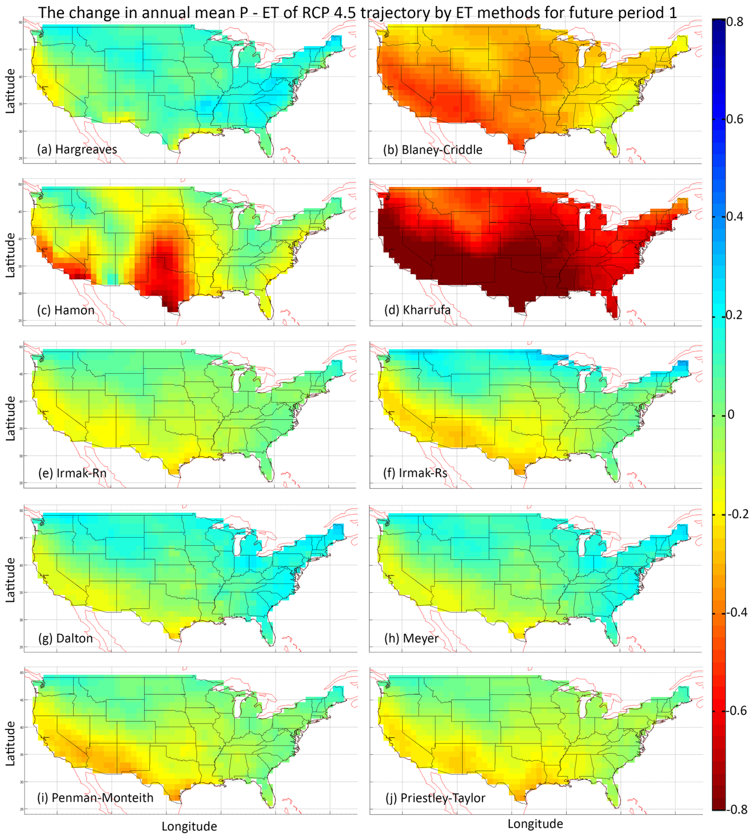

Figure 8. The change in the annual mean P–ET of RCP 4.5 scenario by 10 different evapotranspiration methods. All units are mm day^{-1} and the change is defined as the mean of 2030–2060 minus that of 1950–2005. (All results are interpolated to 1° × 1° grids and averaged over 9 different GCMs).

HESSD
doi:10.5194/hess-2015-408

Title Page
Abstract | Introduction
Conclusions | References
Tables | Figures
◀ | ▶
Back | Close
Full Screen / Esc
Printer-friendly Version
Interactive Discussion

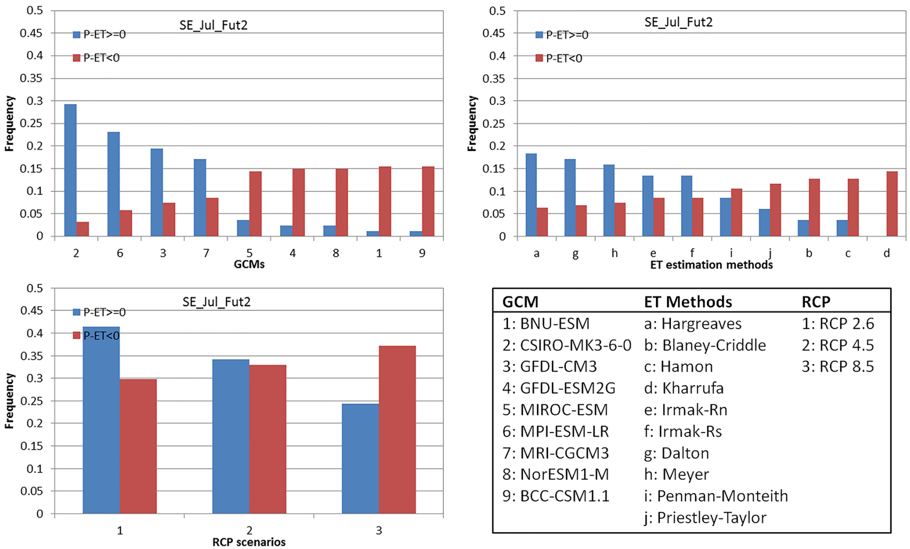

GCM	ET Methods	RCP
1: BNU-ESM	a: Hargreaves	1: RCP 2.6
2: CSIRO-MK3-6-0	b: Blaney-Criddle	2: RCP 4.5
3: GFDL-CM3	c: Hamon	3: RCP 8.5
4: GFDL-ESM2G	d: Kharrufa	
5: MIROC-ESM	e: Irmak-Rn	
6: MPI-ESM-LR	f: Irmak-Rs	
7: MRI-CGCM3	g: Dalton	
8: NorESM1-M	h: Meyer	
9: BCC-CSM1.1	i: Penman-Monteith	
	j: Priestley-Taylor	

Figure 9. Histograms for projected future 2 wet conditions and dry conditions in the Southeast US by GCM, ET method and RCP trajectory for the month of July.

HESSD
doi:10.5194/hess-2015-408

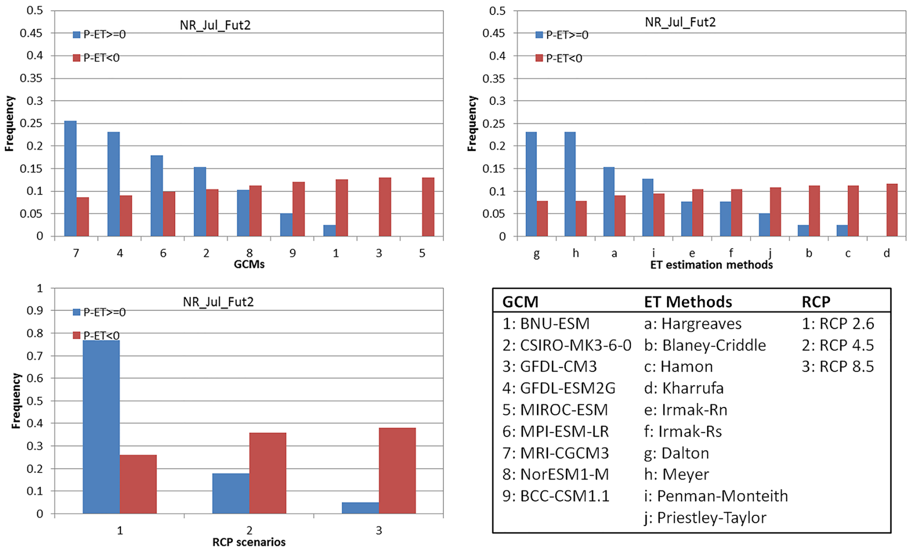

GCM	ET Methods	RCP
1: BNU-ESM	a: Hargreaves	1: RCP 2.6
2: CSIRO-MK3-6-0	b: Blaney-Criddle	2: RCP 4.5
3: GFDL-CM3	c: Hamon	3: RCP 8.5
4: GFDL-ESM2G	d: Kharrufa	
5: MIROC-ESM	e: Irmak-Rn	
6: MPI-ESM-LR	f: Irmak-Rs	
7: MRI-CGCM3	g: Dalton	
8: NorESM1-M	h: Meyer	
9: BCC-CSM1.1	i: Penman-Monteith	
	j: Priestley-Taylor	

Figure 10. Histograms for projected future 2 wet conditions and dry conditions in the Northern Rockies and Plains US by GCM, ET method and RCP trajectory for the month of July.

HESSD
doi:10.5194/hess-2015-408

Sensitivity of future water availability projections to Global Climate Model

S. Chang et al.